Design and validation of a hybrid MPPT algorithm for PVS using an interleaved boost converter

Luis E. Hernandez-Aguilar, *Member, IEEE,* Gerardo Vazquez-Guzman, *Senior Member, IEEE,* Panfilo R. Martinez-Rodriguez, *Senior Member, IEEE,* and Dalyndha Aztatzi-Pluma

***Abstract*—Photovoltaic systems must be highly efficient to transfer the electric power generated to the local loads or to the electrical grid. In partial-shading conditions there are multiple local maximum power points which are not evaluated by conventional MPPT methods producing low efficiency in the photovoltaic system. In this paper a hybrid Particle Swarm Optimization (PSO) based method is proposed. The proposed method allows to locate the global maximum power point enhancing the availability of the generated electrical power and reducing the convergence time compared to the conventional PSO algorithm. The proposed method is compared with classical MPPT algorithms like Hill Climbing (HC), perturb and observe (P&O), incremental conductance (IncCond) and the conventional particle swarm optimization (PSO) method. The comparison is performed by means of numerical simulations and implementing an experimental platform with real photovoltaic panels.**

Link to graphical and video abstracts, and to code: https://latamt.ieeer9.org/index.php/transactions/article/view/9715

***Index Terms*—DC-DC converter, MPPT algorithm, photovoltaic system**

I. Introduction

THE electrical generation by conventional methods contributes significantly to greenhouse gas emissions, therefore, one of the main objectives worldwide is to reduce its environmental impact [1]. As a result, the production of electricity from renewable energy sources, such as solar, hydro and wind power, has become very important in recent decades [2]. In fact, solar energy is expected to be one of the fastest growing, in particular, and in an optimistic scenario the photovoltaic market is expected to witness a remarkable growth in 2026 of around 617 GW of photovoltaic energy [3].

The electrical behavior of a photovoltaic (PV) panel can be characterized by a power-voltage nonlinear curve as it is shown in Fig. 1. Note that, there is an operating point at which the maximum possible power is extracted from the PV panel which is called Maximum Power Point (MPP). The MPP depends on certain environmental conditions, such as irradiance on the PV panel, temperature and shading conditions. Hence, the MPP is never constant along the time, as shown in Fig. 1, [4]–[6]. Constant operation in MPP means maximum energy and economic use of each PV panel [4], [7]. Therefore, several algorithms have been developed in the literature to maintain the operation at this point [4]–[6]. Among these methods are the following: Hill Climbing (HC) [8], perturb and observe (P&O) [9], incremental conductance (IncCond) [10], fractional voltage (Voc) [11], fuzzy logic control (FLC) [12], particle swarm optimization (PSO) [9], among others. The most widely used Maximum Power Point Tracking (MPPT) algorithms are the P&O and IncCond methods due to their simplicity and low cost, although under certain operating conditions, such as partial shading, they do not guarantee accurate tracking of the maximum power point [13]. In contrast, intelligent prediction-based methods, such as meta-heuristic algorithms, can effectively track the MPP under these conditions; one commonly used is the PSO algorithm [9], [13] which, for instance, can accelerate the response speed of the system.

Although PV panels can independently generate electrical power, a system is needed to control and maintain the power generated for future transfer or storage [4]. This is generally done with a DC-DC converter controlled by an MPPT algorithm [14]–[16]. The input is connected directly to the output of the PV panel and its output is connected to a battery for a standalone system, or to an inverter stage for a grid connected system [4], [17], as shown in Fig. 2. Here, the MPPT algorithm commonly operates by sensing voltage and current from the PV panel. The algorithm is responsible for varying the duty cycle of the converter, which means that the operating point is adjusted toward the MPP. Several DC-DC converter topologies are used to solve the MPPT issue, distinguishing between isolated and non-isolated topologies. Isolated topologies reduce the efficiency of the system, which is undesirable since the objective is to take advantage of the maximum available power, while non isolated topologies have higher efficiency but lower gain [14], [16]. So, focusing on the issue of efficiency with greater simplicity of implementation and control, it is feasible to use a non isolated DC-DC converter. Among the main topologies used are the Boost converter [18], the Buck-Boost converter [19], the Cuk converter [20], SEPIC [21] and the Boost-

The associate editor coordinating the review of this manuscript and approving it for publication was Diego Rivelino Espinoza Trejo (*Corresponding author: Gerardo Vazquez-Guzman*).

This work was supported by the TecNM-ITESI and Facultad de Ciencias-UASLP and with the financial support of the Consejo Nacional de Humanidades, Ciencias y Tecnológias (Conahcyt).

L. E. Hernandez-Aguilar is with Tecnologico Nacional de Mexico de Irapuato, (e-mail: enriquehdz@ieee.org).

Gerardo Vazquez-Guzman, and P. R. Martinez-Rodriguez are with the Universidad Autonoma de San Luis Potosi (e-mail: gerardo.vazquez@ieee.org, and pamartinez@ieee.org).

D. Aztatzi-Pluma is with Tecnologico Nacional de Mexico de Abasolo (e-mail: dalyndha.ap@abasolo.tecnm.mx).

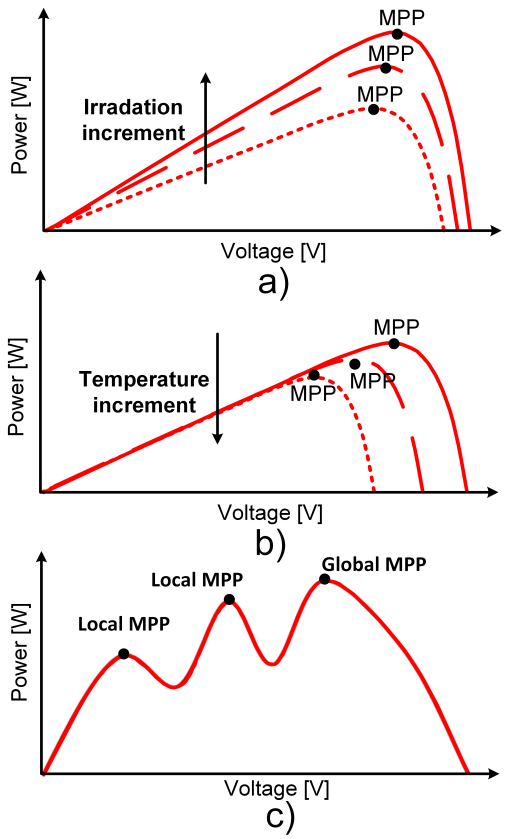

Fig. 1. Power-Voltage curve of a PV panel a) Different levels of irradiance b) different levels of temperature c) shading conditions.

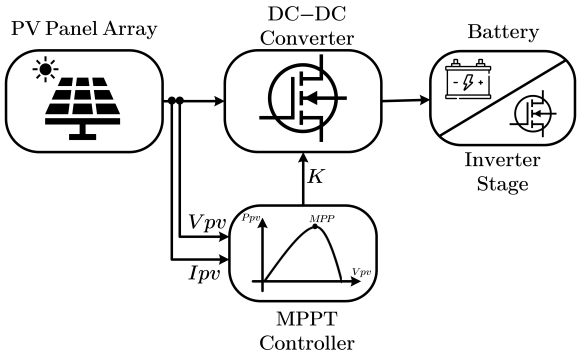

Fig. 2. General block diagram of a PV generation system.

Interleaved converter [22]. The boost converter topology is the most used, nevertheless, it exhibits some drawbacks, for instance, the stress on semiconductors is large, and the input inductor is large to obtain an acceptable current ripple among others. On the other hand, the Buck-boost presents a pulsating input current. Other converter topologies, such as the Cúk or SEPIC present desirable characteristics such as high efficiency and low semiconductor stress, although the high number of components increases the implementation complexity. [14]–[16].

In this work, different MPPT algorithms are assessed including the conventional HC, P&O, IncCond, and an intelligent prediction algorithm such as PSO, which allows tracking under partial shading conditions. All of them under a Boost-Interleaved based experimental platform. The objective is to analyze, by numerical simulations, the tracking efficiency and steady-state error under irradiance variations. Meanwhile, the output power of a PV panel is evaluated experimentally, in a real environment and under partial shading conditions. The rest of the paper is structured as follows; Section II describes the design of the Boost-Interleaved converter for the MPPT; in Section III a description of the selected MPPT methods is presented. In section IV, it is described the procedure and analysis to make the comparison between the selected methods with the help of simulations performed in Simulink. In section V, the experimental implementation based on a Digital Signal Processor (DSP) using a real PV panel is described. In Section VI, discussions and observations regarding the analysis are presented. Finally, in Section VII, the concluding remarks are provided.

II. DC-DC Converter Design

For the evaluation of the MPPT algorithms, the non-isolated Boost-interleaved DC-DC converter is selected due to its superior switching efficiency, reduced semiconductor stress, and lower input current ripple. An additional advantage of this topology is that it does not invert the output voltage polarity, unlike other configurations such as the Cúk and SEPIC converters [14]–[16]. The boost-interleaved converter has been designed based on the boost topology, comprising two branches, each with a switch, an inductor, and a diode. This configuration is shown in Fig. 3. The analysis is performed based on the conventional boost converter topology considering two operating modes of the switch. Therefore, the following design expressions are obtained.

The output voltage of the converter is obtained with,

$$V_o = \frac{1}{1-D} V_i, \tag{1}$$

the inductor value is,

$$L = \frac{V_i D}{\Delta i_L f}. \tag{2}$$

The capacitor value is defined as,

$$C = \frac{D I_o}{\Delta V_o f}. \tag{3}$$

Besides, the current and voltage stress on the switches can be calculated as,

$$I_{pkQ} = \frac{I_o}{1-D} + \frac{V_i D}{2Lf}, \tag{4}$$

$$V_{pkQ} = V_o. \tag{5}$$

For this set of equations, D is defined as the steady-state duty cycle, Δi_L is the ripple of the inductor current, f_{swt} is the switching frequency and ΔV_o is the ripple of the output voltage. As the design of the MPPT algorithms is based on the $P-V$ or $I-V$ curves of the PV panel, then, it is

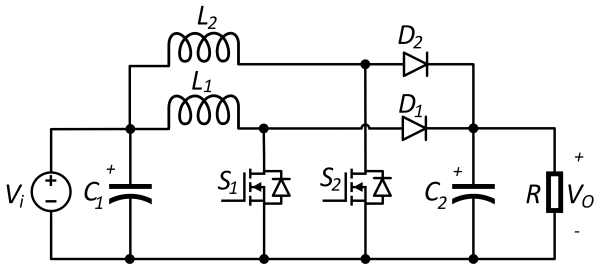

Fig. 3. Simplified circuit of the interleaved-boost converter.

TABLE I
CONVERTER DESIGN VALUES

Parameter	Value
Input voltage V_i	140.8 V
Input current I_i	4.95 A
Output voltage V_o	220 V
Output current I_o	3.182 A
Duty cycle D	36%
Current ripple Δi_L	7%
Voltage ripple ΔV_o	3%
Output power P_o	700 W
Input capacitor C	3.3 μF
Output capacitor C_2	3.3 μF
Inductor of the first switch L_1	3.213 mH
Inductor of the second switch L_2	3.117 mH
Switching frequency f_s	50 kHz
Load resistance R	73 Ω
Diode models D_1 y D_2	IDH16S60C (600V, 16 A)
Switch models Q_1 y Q_2	IRFP460A (500V, 20 A)
S72MC-175 PV panel I_{sc}	5.4 A
S72MC-175 PV panel V_{oc}	45.36 V

considered not necessary to include the dynamical model of the power converter.

The interleaved boost converter is designed for an array of four photovoltaic panels connected in series. Table 1 summarizes the parameters that are considered for the design of the converter. In addition, the design values are presented, as well as the selected switch and diode models. Using these parameters, numerical simulations were performed to validate the design. In particular, the ripples were measured being the magnitude of $\Delta i_{L1} = 316mA$, $\Delta i_{L2} = 326mA$ and the magnitude of the total ripple $\Delta i_{in} = 147mA$ which demonstrates the effective reduction of the input current ripple. The final prototype of the designed interleaved boost converter is shown in Fig. 4, it has six stages: general power supply, power processing, control circuit, current and voltage sensing, relays and communication circuits. It is important to note that the control stage is implemented using a TMS320F28335 DSP from Texas Instruments, which is the platform responsible for processing the MPPT algorithms and generating the control signals.

III. DESCRIPTION OF THE ALGORITHMS

Four MPPT algorithms, namely HC, P&O, IncCond and PSO, are implemented. In addition, a more novel hybrid algorithm, namely PSO/P&O is designed and validated as

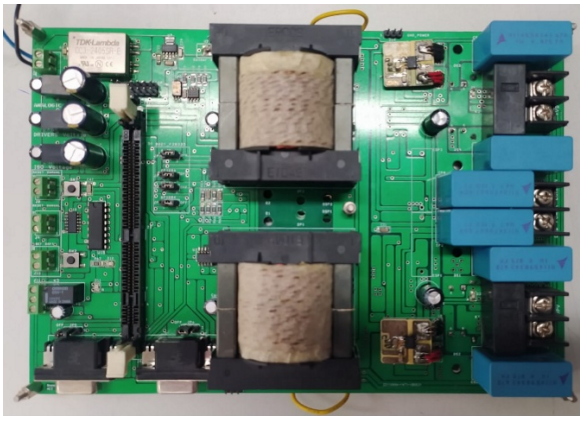

Fig. 4. Experimental prototype of the interleaved boost converter.

the main contribution of this paper. The algorithms are programmed through the TMS320F28335 DSP platform as mentioned before and using the Matlab-Simulink software. The implemented algorithms are described in the next subsections.

A. Hill Climbing (HC)

In order to calculate the power at which the PV panel operates, it is necessary to determine the value of current I_{pv} and voltage V_{pv} presented in the system. Subsequently, the duty cycle perturbations are calculated according to the ratio between the present value of power and its previous value. Fig. 5 illustrates the flow chart of the HC algorithm implemented. The power value of the PV panel is calculated by the product of voltage $V_{pv}(K)$, and current $I_{pv}(K)$. Subsequently, the difference between the present power and the previous one is designated as $DP(K) = P_{pv}(K) - P_{pv}(K-1)$. This signal is the input for the conditional block, wherein three cases are designed. These are as follows:

$if\ (DP(K) == 0)$ – The duty cycle does not change.
$else\ if\ (DP(K) > 0)$ – The duty cycle increment.
$else\ if\ (DP(K) < 0)$ – The duty cycle decrement.

Once the value of the duty cycle has been modified according to the value of the rate of change dD, the power value $P_{pv}(K-1)$ is updated and the next iteration K is performed.

B. Perturb and Observe (P&O)

For this method, as in the HC algorithm, it is essential to determine the operating power of the PV panel by employing the sensed current I_{pv} and voltage values V_{pv}. Then, according to the ratio between the current value of power and voltage and its previous value, the duty cycle disturbances are calculated. Fig. 6 illustrates the flow chart diagram of the P&O algorithm implemented. As in the case of the HC algorithm, the power and the differential power values are calculated which are defined as $P_{pv}(K)$ and $DP(K)$ respectively. For this algorithm, the difference between the current and the previous operating voltage, is defined as $DV(K) = V_{pv}(K) - V_{pv}(K-1)$.

The signal $DP(K)$ is the input of a conditional block, wherein three cases are designed as follows:

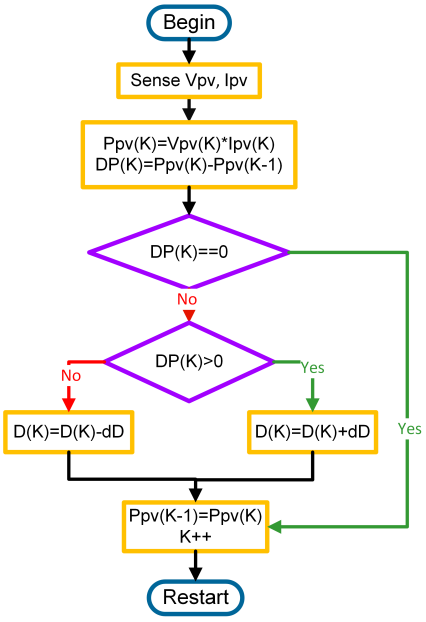

Fig. 5. Flow chart diagram for the HC algorithm.

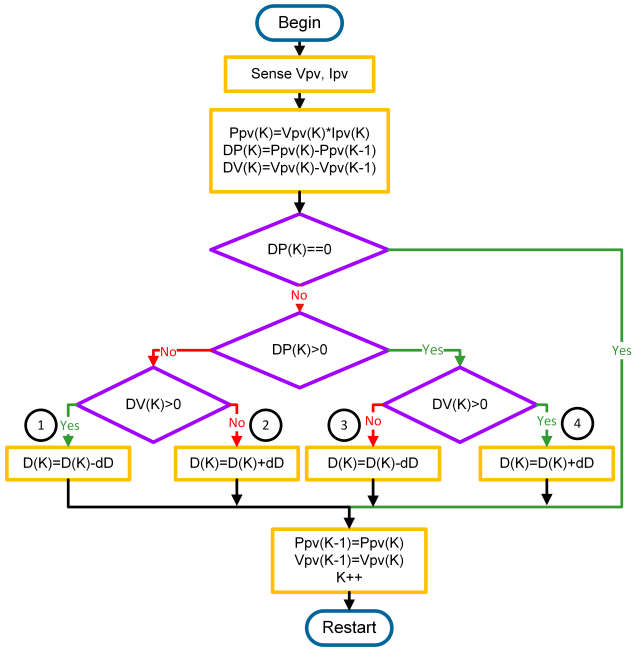

Fig. 6. Flow chart diagram of the P&O algorithm.

$if\ (DP(K) == 0)$ – The duty cycle does not change.
$else\ if\ (DP(K) < 0)$ – Conditional block with cases 1 and 2.
$else\ if\ (DP(K) > 0)$ – Conditional block with cases 3 and 4.

For cases 1 and 2, the signal $DV(K)$ is the input of a conditional block, in which two cases are designed as follows:

$if\ (DV(K) > 0)$ – The duty cycle decrement.
$else\ if\ (DV(K) < 0)$ – The duty cycle increment.

For cases 3 and 4, the signal $DV(K)$ is the input of a conditional block, in which two cases are designed. These are as follows:

$if\ (DV(K) > 0)$ – The duty cycle increment.
$else\ if\ (DV(K) < 0)$ – The duty cycle decrement.

As well as in the HC algorithm, the value of the duty cycle is modified according to the value of the rate of change dD, then, the power value $P_{pv}(K-1)$ and the voltage value $V_{pv}(K-1)$ are updated and the next iteration K is executed.

C. Incremental Conductance (IncCond)

In contrast to the algorithms described before, the MPP tracking in this case depends on the sensed current I_{pv} and voltage values V_{pv}. From these, the instantaneous conductance, given by $G(K) = I_{pv}(K)/V_{pv}(K)$, and the incremental conductance, given by $DG(K) = DI(K)/DV(K)$, are calculated. Subsequently, the duty cycle is modified in accordance with the ratio of the instantaneous conductance $G(K)$ to the incremental conductance $DG(K)$. Fig. 7 shows the flow chart diagram for the implemented IncCond algorithm. As in the P&O algorithm, the differential voltage $DV(K)$ is calculated. Moreover, the difference between the current and the previous operating current, designated as $DI(K) = I_{pv}(K) - I_{pv}(K-1)$ is also calculated. The signal $DV(K)$ is the input of a conditional block, wherein two conditions are designed as follows:

$if\ (DV(K) == 0)$ – First conditional block.
$else\ if\ (DV(K)! = 0)$ – Second conditional block.

For the first conditional block, the signals $DG(K)$ and $G(K)$ are the inputs, where three cases are designed for each variable which are defined as:

$if\ (DG(K) == -G(K))$ – The duty cycle does not change.
$else\ if\ (DG(K) > -G(K))$ – The duty cycle increment.
$else\ if\ (DG(K) < -G(K))$ – The duty cycle decrement.

For the second conditional block, the signal $DI(K)$ is the input, where three cases are designed. These are as follows:

$if\ (DI(K) == 0)$ – The duty cycle does not change.
$else\ if\ (DI(K) > 0)$ – The duty cycle increment.
$else\ if\ (DI(K) < 0)$ – The duty cycle decrement.

As in the previous algorithms, the value of the duty cycle is modified according to the value of the rate of change dD, the voltage value $V_{pv}(K-1)$ and the current value $I_{pv}(K-1)$ are updated and the next iteration K can be performed.

D. Particle Swarm Optimization

The PSO algorithm is programmed based on the values of the present voltage V_{pv} and current I_{pv}, the flow chart diagram is shown in Fig. 8. Initially thirteen particles are defined as i, which correspond to a duty cycle value. The operating power is then measured and stored for each particle as $P(i)$, as well as its duty cycle $D(i)$. Then a loop begins where the power of each particle is compared until the number of particles is greater than 13 $(i > 13)$, while increasing the duty cycle between each iteration. In this way, the particle

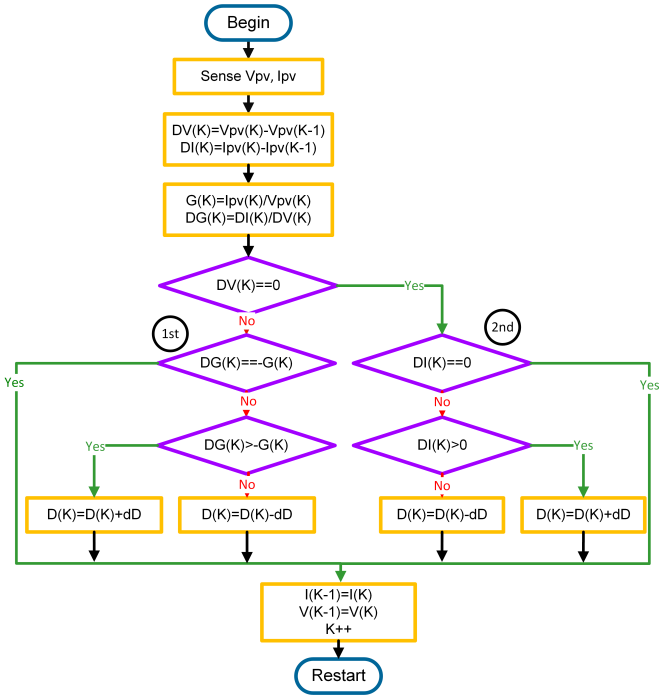

Fig. 7. Programming of the IncCond algorithm.

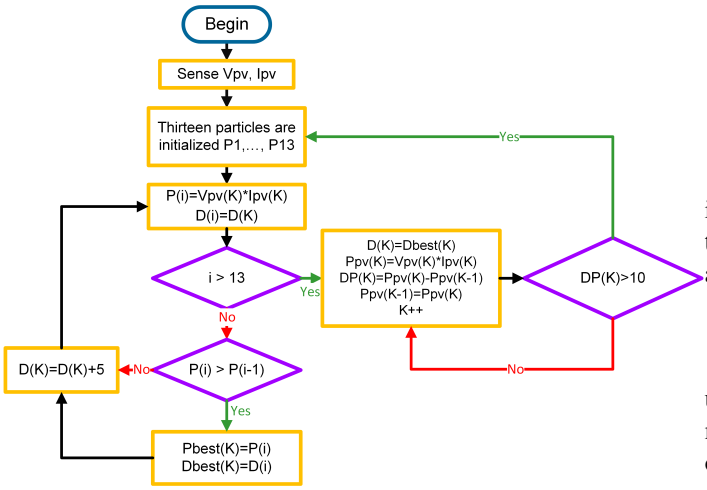

Fig. 8. Programming of the PSO algorithm.

that generates the highest power value is stored as $P_best(K)$, as well as its duty cycle $D_{best}(K)$. At the end of the loop, the duty cycle that generates the highest power is maintained, $DBest(K) = D(K)$, the power value of the PV panel $P_{pv}(K)$ is calculated, as well as the power differential $DP(K)$, until a change in the power differential greater than 10 W is detected $DP(K) > 10$. When this occurs, the algorithm is restarted and the measurement of each particle starts again.

E. Particle Swarm Optimization/Perturb and Observe

The method designed for this algorithm can be described as follows: first, the PSO algorithm is applied to identify the optimal duty cycle, which is advantageous for operation un der partial shading conditions. Subsequently, when the ideal cycle is identified, the P&O algorithm is activated with a reduced duty cycle step, which serves to mitigate unwanted oscillations and reduce the settling time. The algorithm remains in operation until a significant power change is identified, which may be attributed to an abrupt change of irradiance or partial shading. Thereafter, the PSO algorithm is initiated until the optimal duty cycle is determined again.

This algorithm is programmed based on the detected voltage V_{pv} and current I_{pv} values, its flow chart diagram is shown in Fig. 9. The stage of the PSO algorithm is identical to that of the algorithm described in the Subsection III-D; however, only seven particles are initialized so the loop ends until the number of particles is greater than 7 ($i > 7$). This approach enables the reduction of the time required to identify the optimal operating point by approximately 50%.

Subsequently, the P&O algorithm is enabled, beginning with the duty cycle value derived from the PSO algorithm, designated as $P_{best}(K)$. Then the power value of the PV panel $P_{pv}(K)$ is calculated, as well as the power differential $DP(K)$ and the voltage differential $DV(K)$ values. According to the value of the signals $DP(K)$ and $DV(K)$ there are three cases to be consider:

- If changes in $DP(K)$ and $DV(K)$ are both positive or negative, the duty cycle value increases.
- If changes in $DP(K)$ and $DV(K)$ are one positive and the other negative, or vice versa, the duty cycle value is reduced.
- If the chage of $DP(K)$ is equal to zero, the duty cycle remains unchanged.

As well as in the P&O algorithm, the value of the duty cycle is modified according to the value of the rate of change dD, the power value $P_{pv}(K-1)$ and the voltage value $V_{pv}(K-1)$ are updated and the next iteration K is executed.

IV. Simulations Results

The PV panel and the power converter model are simulated using Simulink. The PV panel is simulated using a circuit model of a Solartec S72MC-180 device. The characteristics of the simulated converter are detailed in Table I.

The test pattern proposed by [4] serves as the model for this study. This pattern enables the determination of the ability of the MPPT algorithm to operate in the presence of gradual and sudden fluctuations in irradiance, as well as steady-state conditions; this is presented in Fig. 10. The minimum irradiance considered is $300W/m^2$, the mean value is $600W/m^2$, and the maximum is defined as $900W/m^2$ during a time interval of 8-second with abrupt irradiance variations for PSO and PSO/P&O algorithms and with smooth irradiance variations for HC, P&O and IncCond algorithms. The selection of these two irradiance profiles serves a dual purpose: first, to evaluate the robustness of the proposed algorithm, and second, to avoid operating conditions under which classical MPPT algorithms fail to perform effectively.

Fig. 11 shows the tracking of the maximum power point of each algorithm implemented. The red trace represents the maximum power according to the irradiance pattern, while the purple trace shows the power obtained by the HC algorithm, the blue trace for the P&O algorithm, yellow trace

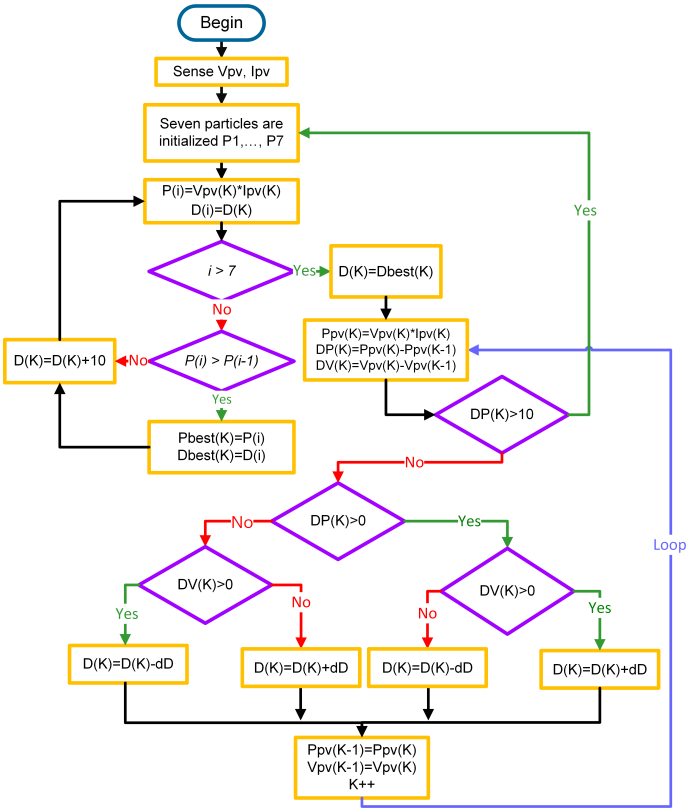

Fig. 9. Programming of PSO/P&O hybrid algorithm.

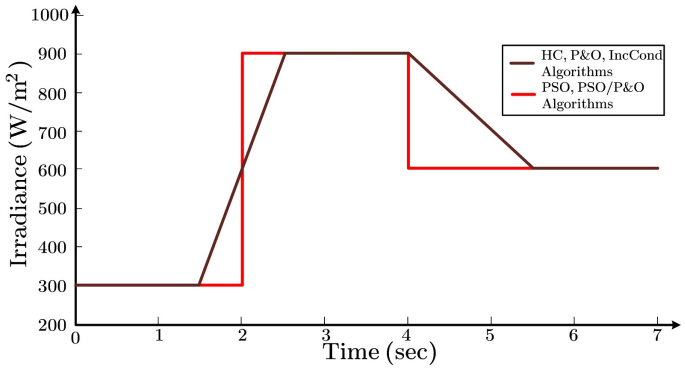

Fig. 10. Irradiance pattern to test the MPPT algorithms.

for the IncCond algorithm, the brown trace for the PSO algorithm and the green trace for the PSO/P&O algorithm. In the case of conventional algorithms, a similar steady-state error is demonstrated. The IncCond algorithm exhibits superior tracking during periods of higher irradiance, while the HC algorithm demonstrates superior tracking during medium irradiance conditions. In contrast, the P&O algorithm, shows reduced steady-state error but increased oscillations during the three irradiance intervals, which can significantly reduce tracking efficiency. For intelligent prediction algorithms, the PSO algorithm exhibited a reduced steady-state error, with the exception of the interval with a lower irradiance. The results demonstrate that the proposed PSO/P&O algorithm provides a reduced steady-state error for the three irradiance intervals. However, it exhibits higher oscillations during irradiance fluctuations in comparison with the PSO algorithm. These results are summarized quantitatively later in the discussion section, including a comparison between efficiency and deviation error for each algorithm.

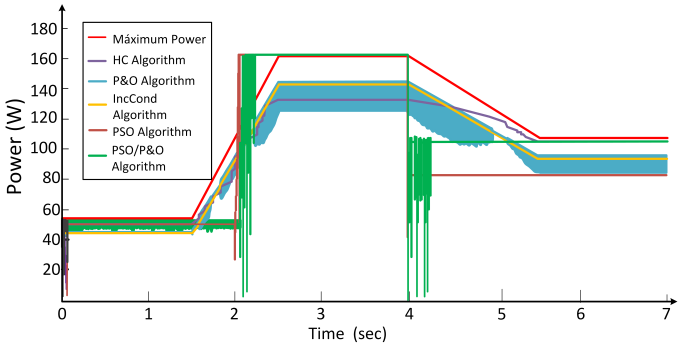

Fig. 11. MPPT of each algorithm implemented by numerical simulations.

V. Experimental Results

The experimental platform is mainly implemented with the Solartec S72MC-180 photovoltaic panel and the interleaved DC-DC boost converter prototype. The experiments are conducted during the month of august between 11:00 a.m. and 12:00 p.m., with an average ambient temperature of 28°C. Moreover, partial shading conditions are also simulated by uniformly covering certain number of cells of the PV panel. Note that, the dynamic behavior of V and I were subject to the environmental conditions and how fast the partial shading was implemented, namely, a wide range of power and irradiance conditions were covered. Fig. 12 shows the experimental tracking of the maximum power point of each algorithm under different shading conditions. The purple trace represents the power obtained by the HC algorithm, the blue trace represents the P&O algorithm, the yellow trace is the result of the IncCond algorithm, the brown trace is the PSO algorithm and finally the green trace corresponds to the PSO/P&O algorithm.

In general, it has been observed that under conditions without partial shading, conventional algorithms attempt to track the MPP. The IncCond algorithm generates higher power in comparison, while the HC algorithm generates the lowest power. On the other hand, intelligent prediction algorithms demonstrate that the proposed PSO/P&O algorithm generates the highest power. Additionally, the settling time is halved compared to the PSO algorithm. In contrast, under 4-cell shading conditions, it is evident that the proposed PSO/P&O algorithm and the PSO intelligent prediction algorithm generate higher power compared to conventional algorithms. However, the proposed algorithm settles in a shorter time and exhibits less oscillations compared to PSO, which may lead to higher tracking efficiency. This behavior is consistently observed under 8-cell shading conditions, the conventional algorithms generate a lower amount of power, while the proposed algorithm generates more power, with a shorter settling time and with a lower power oscillations. These results are presented quantitatively in the discussion section, by means of

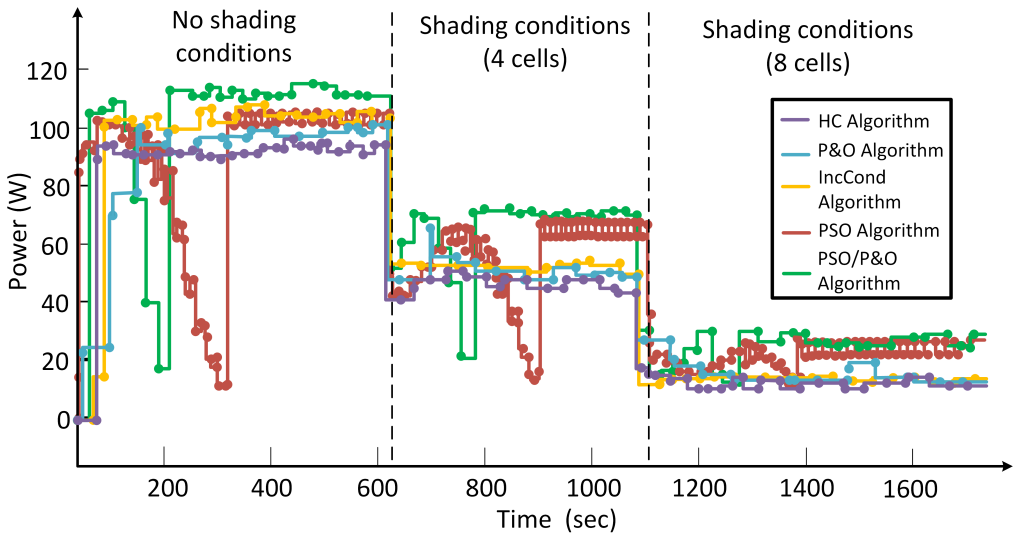

Fig. 12. Experimental results of the tracking of the maximum power point of each algorithm.

TABLE II
QUANTITATIVE COMPARISON OF THE SIMULATION RESULTS

Parameter	MPPT Algorithms				
	HC	P&O	IncCond	PSO	PSO/P&O
Average efficiency	89.8%	84.4%	87.4%	92.4%	97.1%
Average deviation	13.1W	17.8W	14.4W	9.9W	3.9W

TABLE III
QUANTITATIVE COMPARISON OF THE EXPERIMENTAL RESULTS

MPPT Algorithm	Shading Conditions		
	No shading	4 cells	8 cells
HC Algorithm	95 W	46 W	11 W
P&O Algorithm	98 W	50 W	13 W
IncCond Algorithm	105 W	52 W	13 W
PSO Algorithm	104 W	67 W	24 W
PSO/P&O Algorithm	113 W	70 W	28 W

a comparison between the power generated for each evaluated algorithm.

VI. DISCUSSION

The quantitative comparison of the simulation results obtained for the selected MPPT algorithms is shown in Table II. It is observed that conventional algorithms have an efficiency lower than 90% and power losses greater than 10 W. The HC algorithm is the one that presents better tracking regarding these three. However, both the PSO intelligent prediction algorithm and the proposed hybrid PSO/P&O algorithm have shown an efficiency greater than 90%. The proposed algorithm demonstrated the potential to reduce power losses by up to 6 W compared to the PSO algorithm and by approximately 10 W compared to conventional methods.

On the other hand, a quantitative comparison regarding extracted power of the experimental results obtained for the selected MPPT algorithms is shown in Table III. A general observation of the results indicates that the proposed hybrid algorithm consistently generates a higher power output under all operating conditions. Specifically, under unshaded conditions, the proposed algorithm generates a power output that exceeds 8 W compared to conventional algorithms and 9 W compared to the PSO algorithm. Under 4-cell partial shading conditions, the proposed algorithm generates a power greater than 18 W compared to the conventional algorithms and 3 W compared to the PSO algorithm. Finally, under 8-cell partial shading conditions, the proposed algorithm generates a power greater than 15 W compared to the conventional algorithms and 4 W regarding to the PSO algorithm.

In addition, Table IV presents a comparative analysis between the most currently used MPPT algorithms [4], [5], [13] and the proposed hybrid algorithm. The present study analyzes several of the criteria to be considered for its implementation, such as its relative cost, complexity, sensed parameters, and memory requirements. These criteria are considered in the context of its implementation in a digital system, such as a microcontroller or a digital signal processor (DSP). As demonstrated, the proposed algorithm exhibits certain advantages over conventional algorithms, such as HC, P&O, and IncCond. The most significant benefit is its capacity to function under partial shading conditions and achieve enhanced tracking accuracy. In consideration of the more novel algorithms, it has been demonstrated that the proposed algorithm is less complex and requires less memory processing in comparison to the FLC. Furthermore, it has been shown that a shorter response time is achieved in comparison with the PSO algorithm.

Finally, Table V presents a particular comparative analysis between the proposed hybrid algorithm and the native ones,

TABLE IV
COMPARISON IN RECENT TRENDS OF MPPT ALGORITHMS

Criteria	HC	P&O	IncCond	PSO	FLC	PSO/P&O (Proposed)
PV cell dependency	No	No	Yes	No	No	No
Convergence speed	Fast	Fast	Medium	Low	Low	Medium
Tracking accuracy	Low	Low	Medium	High	High	High
MPP oscillations	Medium	Medium	Low	Low	Low	Low
Sensed parameters	*V, I*	*V, I*	*V, I*	*V, I*	*V, I*	*V, I*
Complexity	Low	Low	Medium	Medium	High	Medium
Analog/digital	Both	Both	Digital	Digital	Digital	Digital
Implementation cost	Low	Low	Moderate	Moderate	Moderate	Moderate
Partial shading	No	No	No	Yes	Yes	Yes
Memory requirements	Low	Low	Medium	Medium	Medium	Medium
Response time	*10-50 s*	*60-100 s*	*20-70 a*	*300-350 s*	*250-400 s*	*150-200 s*

TABLE V
COMPARATIVE ANALYSIS BETWEEN PROPOSED AND NATIVE ALGORITHMS

Parameter	P&O	PSO	PSO/P&O (Proposed)	Improvement
Tracking efficiency	84.4%	92.4%	97.1%	+4.7% vs PSO, +12.7% vs P&O
Convergence time	60-100s	300-500 s	150-200 s	2× faster than PSO
Steady state error	17.8 W	9.9 W	3.9 W	60% lower than PSO
Oscillations at MPP	High	Medium	Low	Better stability
Partial shading	Fails	Works	Works	50% faster convergence than PSO

where, according with the parameters defined as tracking efficiency, convergence time, etc., the combined hybrid method presented in this paper results advantageous extracting the best of the original methods.

VII. CONCLUSION

According to the simulation results the proposed hybrid algorithm was the one with the highest efficiency and the lowest power loss under abrupt irradiance changes compared to the PSO algorithm. In addition, for conventional algorithms, it is shown that the HC algorithm had a higher tracking efficiency due to its tracking speed under irradiance variations. On the other hand, for the experimental analysis, the conventional algorithms operate in a very similar way, being the IncCond algorithm the one with the highest power values obtained. However, the HC algorithm had a shorter convergence time, which can be useful under abrupt irradiance variations. Likewise, it was observed that the PSO algorithm tracks similarly to the previous ones under unshaded conditions, but its convergence time increases, making it inefficient under uniform irradiance conditions. However, the proposed hybrid algorithm reduces this convergence time and allows for greater power extraction compared to the other algorithms. In contrast, under shading conditions, it was evident that the PSO algorithm and the proposed hybrid algorithm effectively extract more power. This is reasonable, considering that conventional algorithms were unable to track the maximum optimal power point under these conditions. Considering this, the PSO algorithm extracts a similar power regarding the proposed algorithm; however, it exhibited higher oscillations and a longer convergence time. Therefore, the hybrid PSO/P&O algorithm effectively addresses these limitations, making it suitable for photovoltaic applications.

REFERENCES

[1] UN. *Sustainable Development Objective*. United Nations Organization. USA. 2024. https://sdgs.un.org/.

[2] UN. *Action Climate*. United Nations Organization. USA. 2024. https://sdgs.un.org/.

[3] Solar Power Europe (2023) *Global Market Outlook For Solar Power 2023-2027*. Belgium. 2022. http://www.solarpowereurope.org/.

[4] A. Canchola, G. Vazquez, J. Sosa, P. Martinez, and M. Juarez. "Efficiency Based Comparative Analysis of Selected Classical MPPT Methods," in *IEEE International Autumn Meeting on Power, Electronics and Computing (ROPEC)*, Ixtapa, México, pp. 1-6, 2017. DOI: 10.1109/ROPEC.2017.8261657.

[5] N. Karami, N. Moubayed and R. Outbib. "General review and classification of different MPPT Techniques," in *Renewable and Sustainable Energy Reviews*, vol. 68, pp. 624-630, 2017. https://doi.org/10.1016/j.rser.2016.09.132.

[6] M. Sarvi, A. Azadian. "A comprehensive review and classified comparision of MPPT algortihms in PV sytems," in *Energy Systems*, vol. 2, no. 13, pp. 281-320, 2021 https://doi.org/10.1007/s12667-021-00427-x.

[7] F. Tahiri, K. Chikh, M. Khafallah, and A. Saad. "Comparative study between two Maximum Power Point Tracking techniques for photovoltaic system," in *International Conference on Electrical and Information Technologies (ICEIT)*, Tangiers, pp. 10, 2016. DOI: 10.1109/EITech.2016.7519571.

[8] V. Jately, et. al. "Experimental Analysis of hill-climbing MPPT algorithms under low irradiance levels," in *Renewable and Sustainable Energy Reviews*, vol. 150, p. 111467, 2021. https://doi.org/10.1016/j.rser.2021.111467.

[9] S. Figueiredo and R. Nayana. "Hybrid MPPT Technique PSO-P&O Applied to Photovoltaic Systems Under Uniform and Partial Shading Conditions," in *IEEE Latin America Transactions*, vol. 19, no. 10, pp. 1610–1617, 2021. DOI: 10.1109/TLA.2021.9477222.

[10] L. Shang, H. Guo and H. Zhu. "An improved MPPT control strategy based on incremental conductance algorithm," in *Protection and Control of Modern Power Systems*, vol. 5, no. 2, pp. 1-8, 2020. https://doi.org/10.1186/s41601-020-00161-z.

[11] A. Hassan, O. Bass, and M. Masoum. "An improved genetic algorithm based fractional open circuit voltage MPPT for solar PV systems," in *Energy Reports* vol. 9, pp. 1535-1548, 2023. https://doi.org/10.1016/j.egyr.2022.12.088.

[12] T. Hassan, et. al. "A novel algorithm for MPPT of an isolated PV system using push pull converter with fuzzy logic controller," in *Energies*, vol. 13, no. 15, p. 4007, 2020. https://doi.org/10.3390/en13154007.

[13] B. Yang, et. al. "Comprehensive overview of maximum power point tracking algorithms of PV systems under partial shading condition," in *Journal of Cleaner Production*, vol. 268, p. 121983, 2020. https://doi.org/10.1016/j.jclepro.2020.121983.

[14] F. Mumtaz, et al. "Review on non-isolated DC-DC converters and their control techniques for renewable energy applications," in *Ain Shams Engineering Journal*, vol. 12, no. 4, pp. 3747-3763, 2021. https://doi.org/10.1016/j.asej.2021.03.022.

[15] B. Revathi, and M. Prabhakar "Non isolated high gain DC-DC converter topologies for PV applications – A comprehensive review," in *Renewable and Sustainable Energy Reviews*, vol. 66, pp. 920-933, 2016. https://doi.org/10.1016/j.rser.2016.08.057.
[16] M. Chewale, R. Wanjari, V. Savakhande, and P. Sonawane "A Review on Isolated and Non-isolated DC-DC Converter for PV Application," in *International Conference on Control, Power, Communication and Computing Technologies (ICCPCCT)*, Kannur, India, pp. 399-404, 2018. DOI: 10.1109/ICCPCCT.2018.8574312.
[17] G. Lepoldo, et al. "Flatness-Based Control for the Maximum Power Point Tracking in a Photovoltaic System," in *Energies*, vol. 12, no. 10, 2019. https://doi.org/10.3390/en12101843.
[18] J. Ingilala, and I. Vairavasundaram. "Investigation of high gain DC/DC converter for solar PV applications," *e-Prime-Advances in Electrical Engineering, Electronics and Energy*, vol. 5, p. 100264, 2023. https://doi.org/10.1016/j.prime.2023.100264.
[19] M. Kaouane, A. Boukhelifa, and A. Cheriti. "Regulated output voltage double switch Buck-Boost converter for photovoltaic energy application," in *International Journal of Hydrogen Energy* , vol. 41, no. 45, pp. 20847-20857, 2016. https://doi.org/10.1016/j.ijhydene.2016.06.140.
[20] J. C. de Morais, J. L. de Morais and R. Gules. "Photovoltaic AC Module Based on a Cuk Converter with a Switched-Inductor Structure," in *IEEE Transactions on Industrial Electronics*, vol. 66, no. 5, pp. 3881-3890, 2019. DOI: 10.1109/TIE.2018.2856202.
[21] J. Ahmad, E. Ismail, and H. Behbehani. "High voltage step-up integrated double Boost-SEPIC-DC-DC converter for fuell-cell and photovoltaic applications," in *Renewable Energy*, vol. 82, pp. 44-53, 2015. https://doi.org/10.1016/j.renene.2014.08.034.
[22] N. Shanthi, et. al. "High Efficient Interleaved Boost Converter for Photovoltaic Applications ," in *2018 Internacional Conference on Computation of Power, Energy, Information and Communication (ICCPEIC)*, vol. 188, pp. 305-309, 2018. DOI: 10.1109/ICCPEIC.2018.8525145.

Luis Enrique Hernández Aguilar (Member, IEEE) Electronics engineer graduated from the Instituto Superior de Irapuato with a specialty in power electronics in 2024. He is currently a master's student in power electronics engineering at the same institute. He has published in congresses such as CIENERGIA, Women's Participation in Science and ROPEC in 2022, with a stay in the electrical engineering department of the Instituto Tecnológico de Morelia. Her research has focused on DC-DC and DC-AC power converters for photovoltaic applications, as well as the implementation of maximum power point tracking algorithms.

Gerardo Vázquez Guzmán received the B.S. degree in electronic engineering from the Technical Institute of Apizaco, Tlaxcala, México, in 2003, the M.S. degree in electronic engineering from the National Center of Research and Technological Development, Cuernavaca, México, in 2006 and the Ph.D. degree in electrical engineering from the Technical University of Catalonia in Barcelona, Spain, in 2013. In 2009, he was a Visiting Scholar at the Aalborg University, Aalborg, Denmark. He is Senior member of the IEEE. From 2012 to 2024 he was a full-time professor with the National Technological of Mexico /Technological Institute of Superior Studies of Irapuato. Since 2025 he has been holding a Professor-Researcher position at the Coordinacion para la Innovacion y Aplicacion de la Ciencia y Tecnologia (CIACyT), Universidad Autonoma de San Luis Potosi, Mexico. His main research interests include the analysis and design of power electronics converters, renewable energy systems and grid connected converters.

Panfilo Raymundo Martínez Rodríguez (Senior Member, IEEE) received the Ph.D. degree in applied science from Instituto Potosino de Investigacion Cientifica y Tecnologica A.C. IPICYT, San Luis Potosi, Mexico, in 2007. He is currently a professor researcher with Facultad de Ciencias, Universidad Autónoma de San Luis Potosí, Mexico. His research interests include power electronics applications and modeling, design, and control of power electronics converters applied to the improvement of the electrical power quality and the electrical energy conversion from non-conventional electrical power sources.

Dalyndha Aztatzi Pluma received the B.S. degree in chemical engineering from the Autonomous University of Tlaxcala, México, in 2007, the M.S. degree in chemical engineering from the Autonomous University of Tlaxcala, Tlaxcala, México, in 2011 and the Ph.D. degree in chemical engineering from the Technological Institute of Celaya, Guanajuato, Mexico, in 2017. In 2019, she was visiting scholar at the University of Guanajuato, Mexico. Since 2020 she joined with the National Technological of Mexico /Technological Institute of Superior Studies of Abasolo holding an associate Professor-Researcher position at the Mechatronic Department. Her research interests include molecular simulation apply to nanomaterials, biocomposites and programming of embedded electronic systems.